Unstructured Grid Euler Method Assessment for Aerodynamic Performance Prediction of the Complete TCA Configuration at Supersonic Cruise Speed

Farhad Ghaffari

Aero– & Gas– Dynamics Division
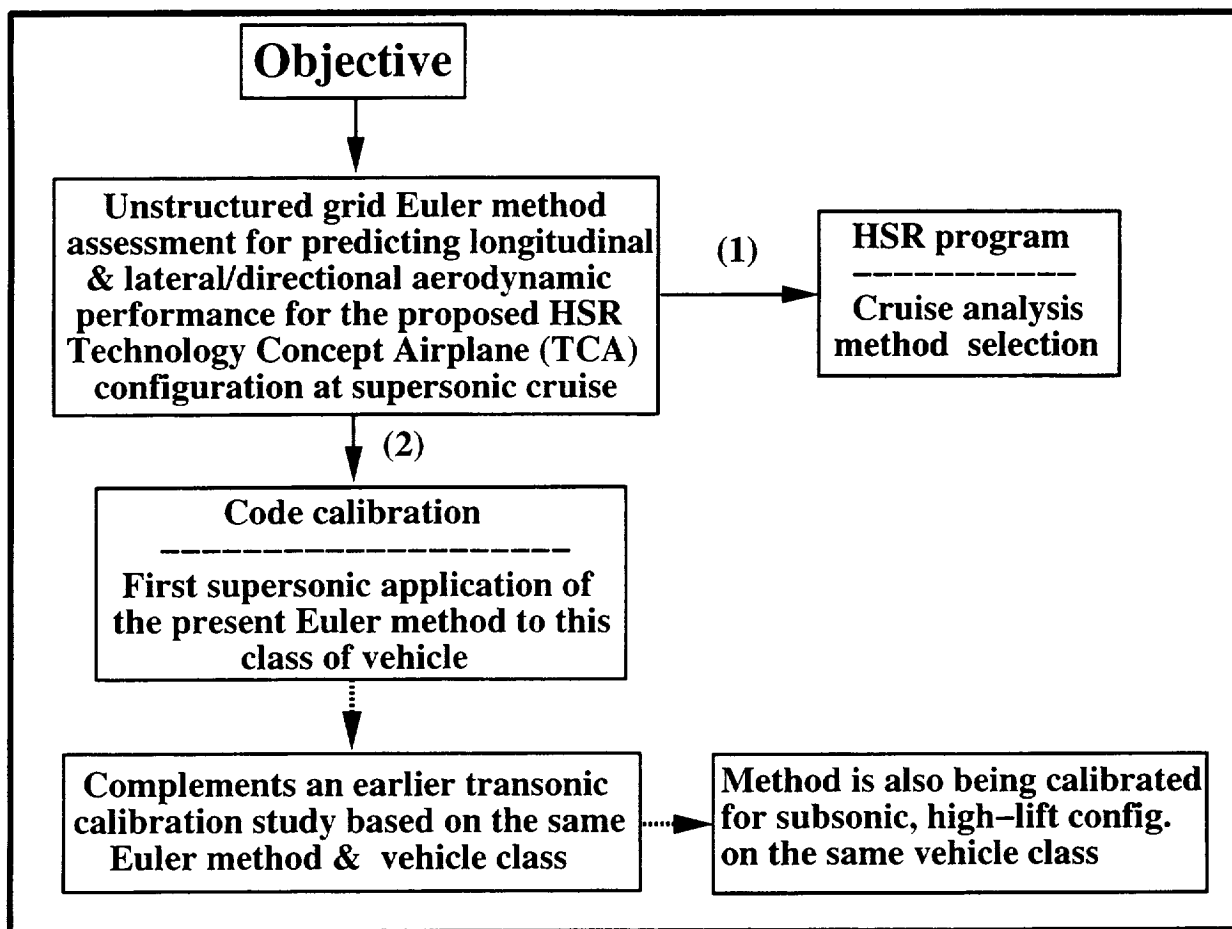### NASA Langley Research Center

High Speed Research Program
Biannual Airframe Technical Review
Los Angeles, February 9–13, 1998

    Unstructured grid Euler computations, performed at supersonic cruise speed, are presented for a proposed high speed civil transport configuration, designated as the Technology Concept Airplane (TCA) within the High Speed Research (HSR) Program. The numerical results are obtained for the complete TCA cruise configuration which includes the wing, fuselage, empennage, diverters, and flow through nacelles at Mach 2.4 for a range of angles–of–attack and sideslip. The computed surface and off–surface flow characteristics are analyzed and the pressure coefficient contours on the wing lower surface are shown to correlate reasonably well with the available pressure sensitive paint results, particularly, for the complex shock wave structures around the nacelles. The predicted longitudinal and lateral/directional performance characteristics are shown to correlate very well with the measured data across the examined range of angles–of–attack and sideslip. The results from the present effort have been documented into a NASA Controlled–Distribution report which is being presently reviewed for publication.

-- OUTLINE --

- **Objective**

- **Computational Approach & Attributes**
  - → Numerical Model Approach
  - → Selected Computational Flow Matrix
  - → Typical Computational Grid
  - → Numerical Method & Typical Convergence

- **Results & Discussion**

  - → Longitudinal Aerodynamic Analysis
  - → Lateral/Directional Aerodynamic Analysis

- **Concluding Remarks**

- **What's Next?**

This chart shows the outline of this presentation.

```
┌─────────────────────────────────────────────────────────────────────────┐
│                          ┌─────────────┐                                  │
│                          │  Objective  │                                  │
│                          └──────┬──────┘                                  │
│                                 ▼                                         │
│  ┌─────────────────────────────────────┐        ┌───────────────────────┐│
│  │  Unstructured grid Euler method      │        │  HSR program          ││
│  │  assessment for predicting longitudinal│ (1)  │  ─────────────────    ││
│  │  & lateral/directional aerodynamic   │───────▶│  Cruise analysis      ││
│  │  performance for the proposed HSR    │        │  method  selection    ││
│  │  Technology Concept Airplane (TCA)   │        └───────────────────────┘│
│  │  configuration at supersonic cruise  │                                 │
│  └─────────────────────────────────────┘                                 │
│                     │ (2)                                                  │
│                     ▼                                                      │
│  ┌─────────────────────────────────────┐                                 │
│  │  Code calibration                    │                                 │
│  │  ─────────────────────────────────   │                                 │
│  │  First supersonic application of     │                                 │
│  │  the present Euler method to this    │                                 │
│  │  class of vehicle                    │                                 │
│  └─────────────────────────────────────┘                                 │
│                     │                                                      │
│                     ▼                                                      │
│  ┌─────────────────────────────────────┐  ┌────────────────────────────┐ │
│  │  Complements an earlier transonic    │  │  Method is also being       │ │
│  │  calibration study based on the same │─▶│  calibrated for subsonic,   │ │
│  │  Euler method &  vehicle class       │  │  high–lift config.          │ │
│  └─────────────────────────────────────┘  │  on the same vehicle class  │ │
│                                            └────────────────────────────┘ │
└─────────────────────────────────────────────────────────────────────────┘
```

The primary objective of the present effort is to evaluate an unstructured grid Euler method for predicting the longitudinal and lateral/directional performance characteristics of the TCA configuration at the design supersonic cruise Mach number of 2.4. Due to the inviscid nature of the present analysis, the evaluation emphasis is placed on the method's ability to predict the aggregate forces and moments acting on the configuration accurately and not necessarily the detail flow physics. In spite of this fact, some representative samples of the predicted flow structures will be presented.

The results from this effort contribute to two activities; 1)– the HSR tools & methods development, where a variety of CFD technologies are being evaluated for their potential utilization in the early phase of the configuration design and aerodynamic analysis, and 2)– the code calibration. The latter code calibration effort at supersonic speed would complement the prior investigations where the aerodynamic prediction capabilities of the same methodology were evaluated at both transonic as well as subsonic speeds for this vehicle class.

Experimental Wind–Tunnel Model and Numerical Model for TCA

Truncated TCA model

Complete TCA model

Mach Line

Mach Angle

Mach Cone

1.675% Scale model LaRC UPWT

Truncated TCA Model | **Complete TCA Numerical Model**
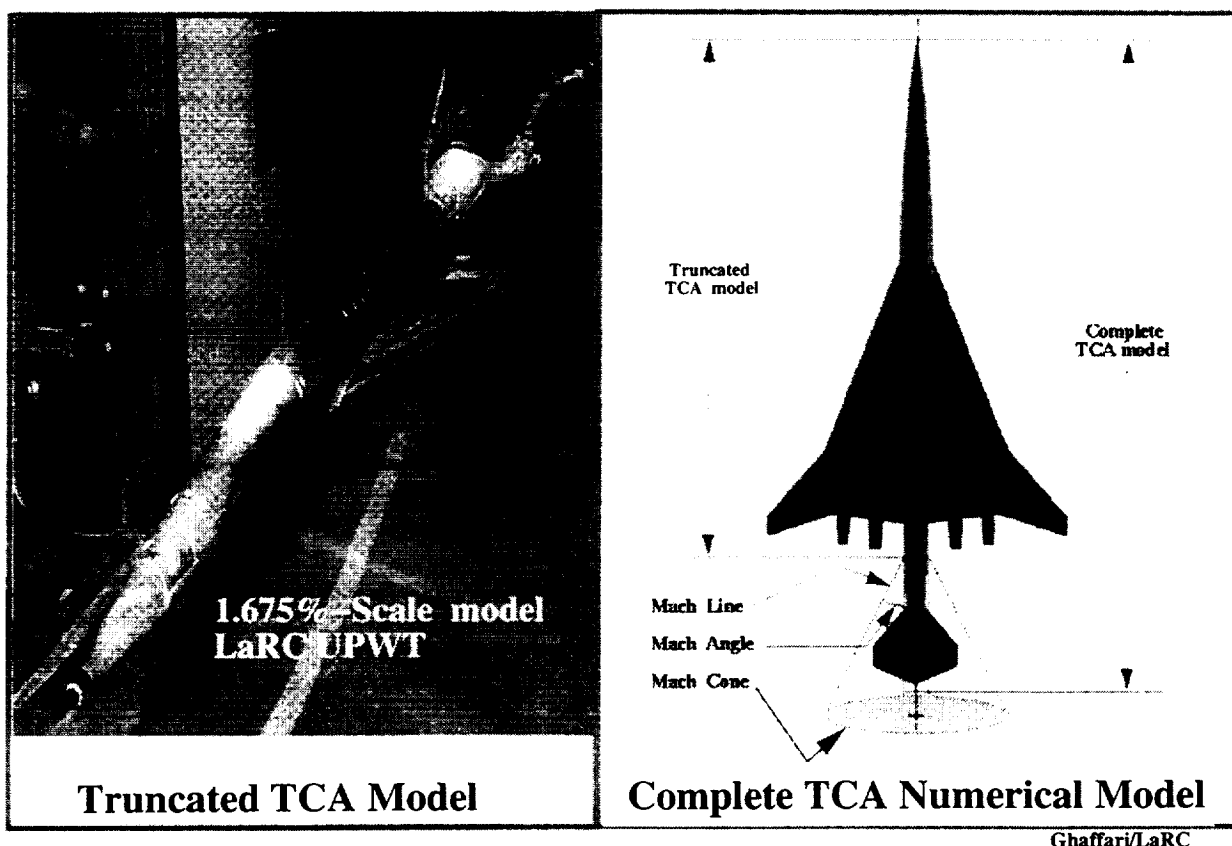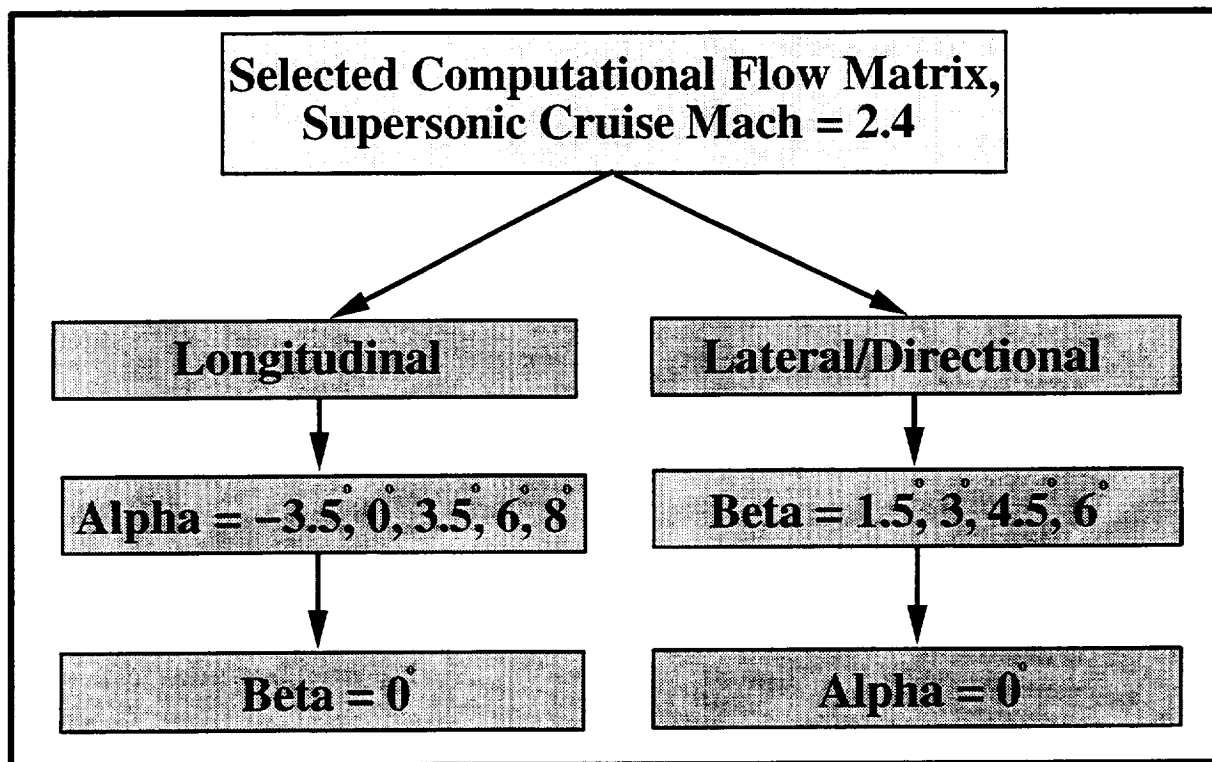
GhaffarI/LaRC

Figure on the left shows a photograph of the sting mounted "truncated TCA model" as installed in the NASA Langley Research Center (LaRC) Unitary Plan Wind Tunnel (UPWT). The truncated (aft–fuselage/empennage removed) TCA model, consisting of wing/fuselage/nacelle/diverter combinations, was primarily tested to obtain the aerodynamic performance data for supersonic cruise conditions. The figure on the right shows the present numerical model including the aft–fuselage/empennage components. Although, the experimental data have been obtained with the truncated TCA model, provision has been made for extracting complementary aerodynamic characteristics from the present numerical analysis of the complete TCA model. This provision is based on an assumption, derived from the fundamental supersonic aerodynamic principle, that simply states that any flow disturbance caused by a source in a supersonic medium does not propagate upstream beyond its Mach cone. Based on this principle, it is assumed in the present numerical approach that any flow disturbance caused by the presence of the empennage is confined to a Mach cone originated from the longitudinal station where the empennage is truncated from the wind tunnel model. The approximate shape of this Mach cone, having a semi–vertex angle of 24.6 degree (i.e., $\sin^{-1}(1/\text{Mach}) = \sin^{-1}(1/2.4) = 24.6$ degree), is schematically shown over the complete TCA numerical model planform in the above figure on the right hand–side.

There are two clear advantages associated with modeling the complete TCA configuration. The obvious advantage is the efficient utilization of the computer resources, i.e., one computational solution provides results for both the complete TCA model and the truncated TCA model. The second advantage is that the computational results for the complete TCA model provide valuable aerodynamic performance predictions for which no experimental data presently exist within the HSR program. Though not presented in this paper, the validity of the computational results for the truncated TCA model, extracted from the complete TCA numerical simulation, have been fully addressed through a set of separate numerical analysis representing the actual sting–mounted truncated TCA model. The latter analysis is included in the final NASA Controlled–Distribution form publication which is presently being reviewed.

Selected Computational Flow Matrix,
Supersonic Cruise Mach = 2.4

Longitudinal

Alpha = -3.5°, 0°, 3.5°, 6°, 8°

Beta = 0°

Lateral/Directional

Beta = 1.5°, 3°, 4.5°, 6°

Alpha = 0°

Preliminary analysis of the available experimental data from UPWT was conducted to identify the conditions for the present numerical investigation.   This chart shows the selected computational matrix for the longitudinal (an alpha sweep at zero sideslip) and lateral/directional (a beta sweep at zero alpha) aerodynamic analysis at the design supersonic cruise Mach number of 2.4.

Computational Grid Domain for the Complete TCA

**Grid sensitivity
study led to:**

# of cells ~ 670,000
# of faces ~ 1,400,000
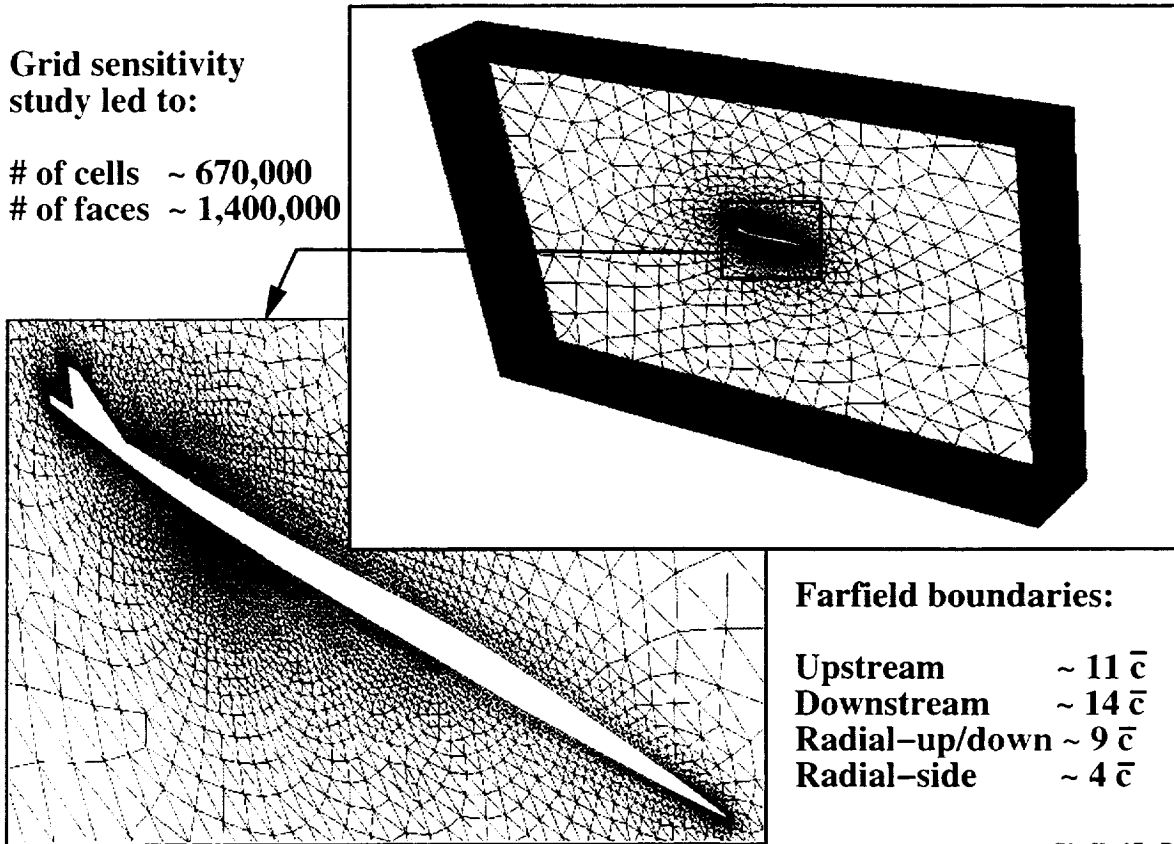
Farfield boundaries:

Upstream ~ 11 $\bar{c}$
Downstream ~ 14 $\bar{c}$
Radial–up/down ~ 9 $\bar{c}$
Radial–side ~ 4 $\bar{c}$

Ghaffari/LaRC

A grid sensitivity analysis was conducted to study the effect of grid resolution on solution convergence and the aerodynamic performance predictions. This analysis indicated that the baseline grid, consisting of about 670,000 cells, was sufficient to simulate the inviscid flow about the complete TCA configuration with the same degree of accuracy as the solutions obtained on a grid that was twice as fine (i.e., about 1.3 million cells). The degree of solution accuracy between the baseline and the fine grid was assessed for the surface and off–surface flow characteristics as well as the integrated forces and moments across the examined range of angle–of–attack (i.e., –3.5, 0, 3.5, 6, and 8 degree). Though not included in this paper, the complete results and analysis from this grid sensitivity study are included in a NASA Controlled–Distribution report which is currently being reviewed for publication.

The above figure shows the farfield boundary faces for the computational domain and the grids in the configuration plane–of–symmetry. The computational domain farfield boundary dimensions are also shown in the above figure as multiples of the wing mean aerodynamic chord ($\bar{c}$). It should be noted that this grid, and in particular the upstream farfield boundary extension, was defined in such a way that it could be used to compute the flow at both supersonic as well as transonic speeds.

Computational Surface Grid for the Complete TCA

Lower surface view

# of triangles ~ 60,000
# of nodes   ~ 30,000
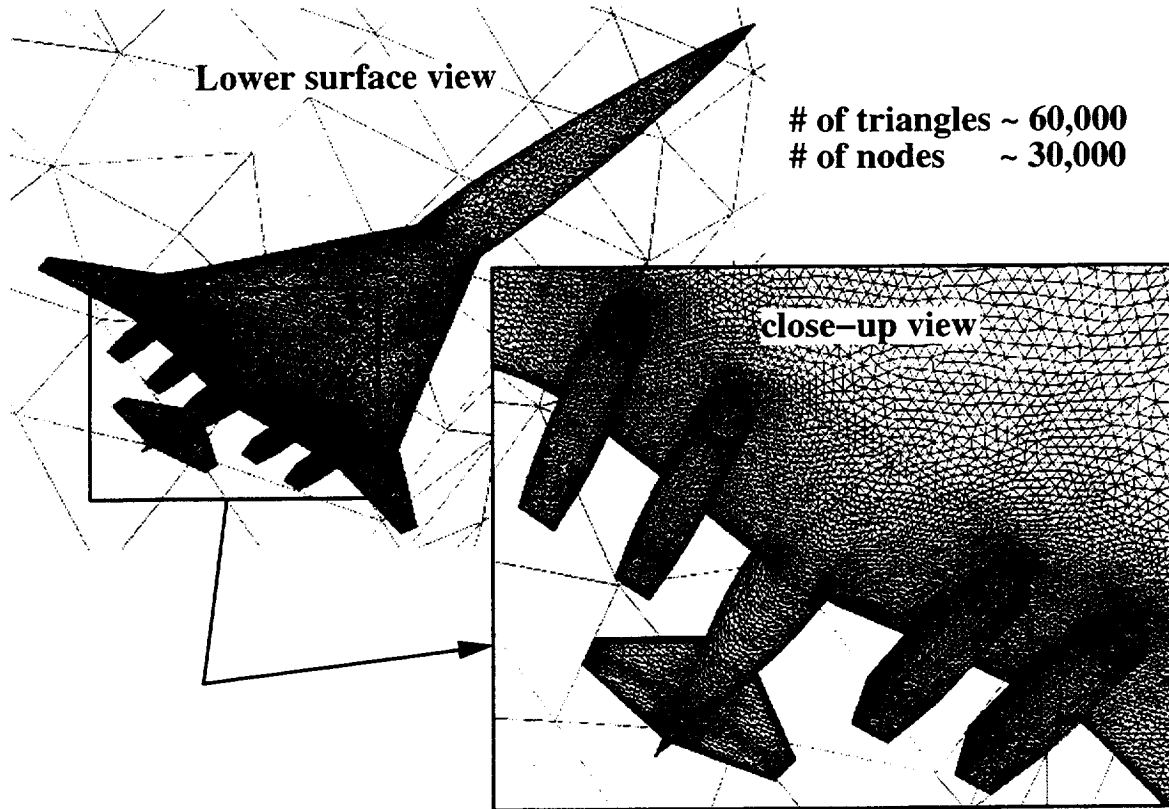
close-up view

GhaffarI/LaRC

This chart shows the lower surface view of the computational grid and a close-up view of the surface triangles around the nacelles. The baseline computational grid consisted of about 60,000 surface triangles to discretize one-half of the complete TCA numerical model. Complementary to the experimental test, the interior surfaces of the nacelles are modelled to simulate flow through propulsion effects.

Computational Methodologies

— TetrUSS —
Developed at NASA Langley Research Center

- ## GridTool
    - o CAD ----> Suface patch
    - o NonUniform Rational B-Spline (NURBS)

- ## VGRID
    - o Surface patch ----> Surface/volume-tetrahedral mesh
    - o Advancing Front Technique

- ## USM3D
    - o Upwind-biased, cell center, finite volume approach
    - o Implicit time integration (Gauss-Siedel)
    - o Convergence acceleration with local time stepping
    - o Flux Difference Splitting approach (Roe's scheme)

- ## VPLOT3D
    - o Solution postprocessing (Not used in this study)

This chart shows the salient features of the computational methodology, known as TetrUSS, which is being evaluated in the present analysis. TetrUSS package includes: GridTool, to discretize primarily the surface geometry; VGRID, to generate flow field grids; USM3D, to solve the flow; and VPLOT3D, to postprocess the solutions (not used in the present analysis).

Convergence Characteristics and Typical Method Performance for Complete TCA

Supersonic cruise configuration; $\beta = 0°$, $M_\infty = 2.4$
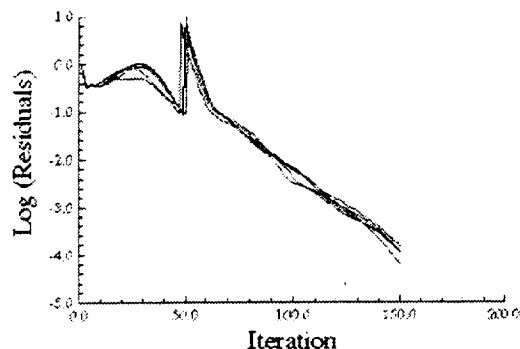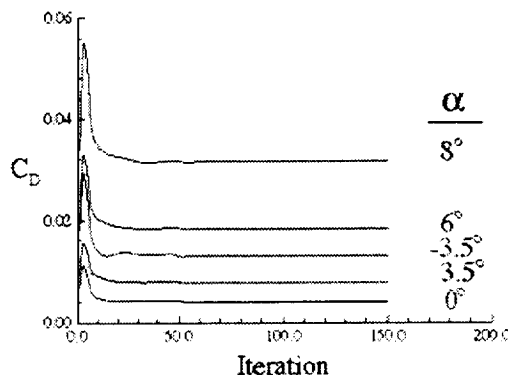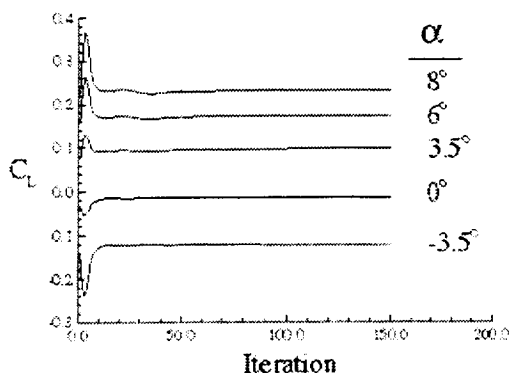
This chart shows the solution convergence characteristics for the complete TCA configuration, using the baseline grid, across the examined range of angles–of–attack. A typical solution convergence for the longitudinal analysis is achieved with about 150 iterations where the total residuals are dropped by approximately 3 to 4 orders of magnitude and reduced the oscillations in lift and drag coefficients to a negligible level. All computations are performed on the Cray–C90 class computer with a typical case requiring about 120–MegaWords of memory and about 1/2–CPU hours to achieve the above nominal convergence characteristics. All solutions are based on second–order, flux–difference–splitting (FDS2) algorithm.

295

-- Results & Discussion --

Longitudinal analysis

- **Typical flow features**
  - Surface pressure contours
  - Correlation with PSP data
  - Off–surface flow structures
- **Force & moment analysis**
  - Drag correction to Euler predictions
  - Correlation with data

Lateral/directional analysis

- **Typical surface pressure contours**
- **Forces & moments predictions – correlation with data**

Longitudinal aerodynamic analysis is presented next which includes results for typical flow features followed by integrated forces/moment analysis and correlations with experimental data.

Surface Cp Prediction for the Complete TCA Configuration

Flow through propulsion cruise geometry; Alpha=3.5°, Mach=2.4

Surface Cp

−0.2   0.2
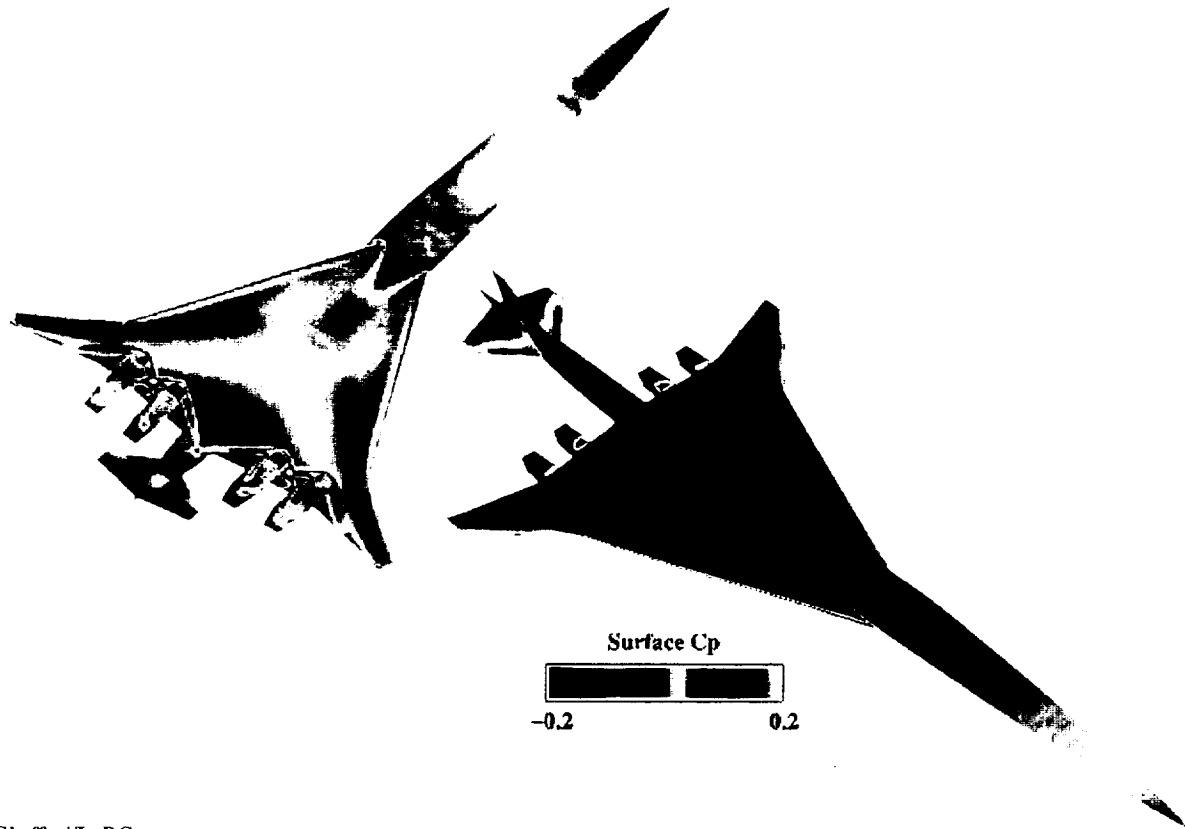
Ghaffari/LaRC

Typical surface Cp distributions computed for the complete TCA configuration are shown here from two different vantage points. The computed lower surface Cp distribution can be characterized by the flow compression around the nose apex region, the inboard/outboard wing leading edges and a complex shock wave structure around the engine nacelles. The shock waves are emanated from both the inboard and the outboard leading–edges of the nacelle diverters. The upper surface Cp contours reveal a fairly benign distribution over the forebody and a region of flow expansion that runs parallel to the inboard wing leading–edge which extends onto the wing outboard panel. The upper surface Cp distribution also indicates a slight flow expansion around the leading edges of the outboard wing, along with a region of compression around the horizontal–tail leading–edges.

297

Surface Cp Prediction for the Complete TCA and Correlation with PSP
Unstructured Grid Method (TetrUSS); M = 2.4, Alpha = 3.5°, R_{ft} = 4 x 10⁶
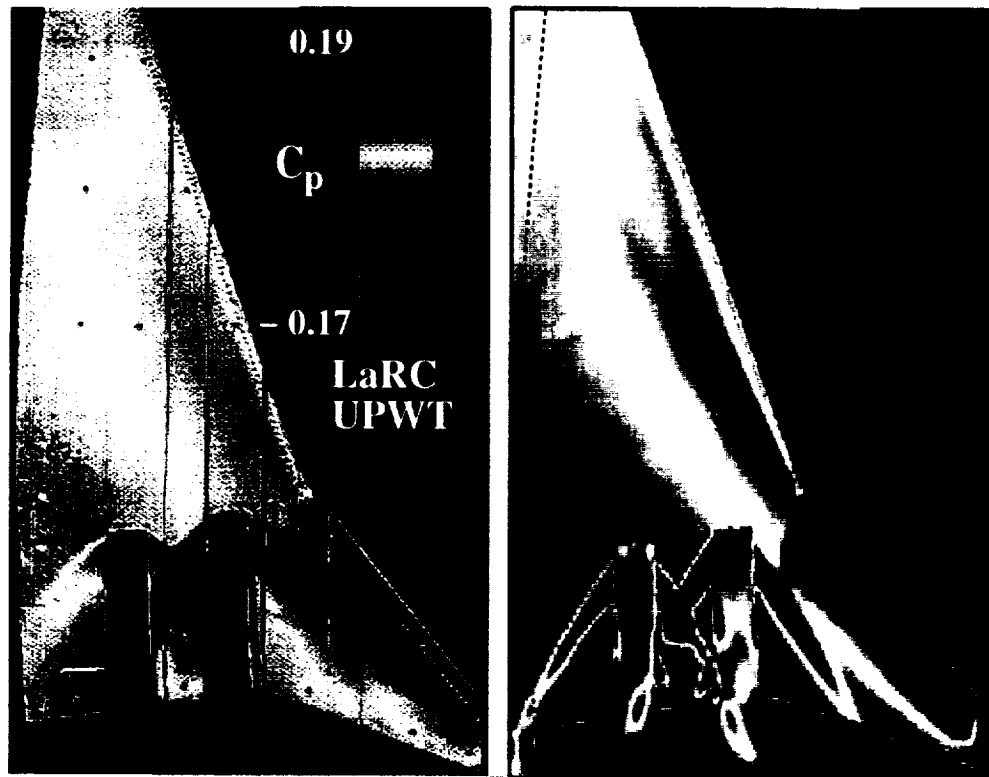
A limited amount of Pressure Sensitive Paint data were acquired on the truncated TCA model during the UPWT test. Typical PSP data obtained over the wing lower–surface of the TCA supersonic cruise configuration (i.e., no–control surface deflection) at 3.5 degree angle–of–attack and Mach number of 2.4 is presented on the left hand–side of the above figure. Complementary to the PSP results, the surface Cp computed for the same configuration and flow conditions is shown from the same vantage point on the right hand–side. The computational result is actually extracted from the same numerical solution that was shown in the previous figure, except the pressure range and the corresponding color map have been changed to match that of the PSP data. The results indicate that the two main flow features highlighted by a region of flow compression under the wing outboard section as well as the complex shock wave structures around the nacelles have been predicted reasonably well. Note that the diffusive nature of the PSP shock waves which are, in general, located further upstream than those of the predictions are attributed to the lack of viscous modelling in the present Euler numerical analyses.
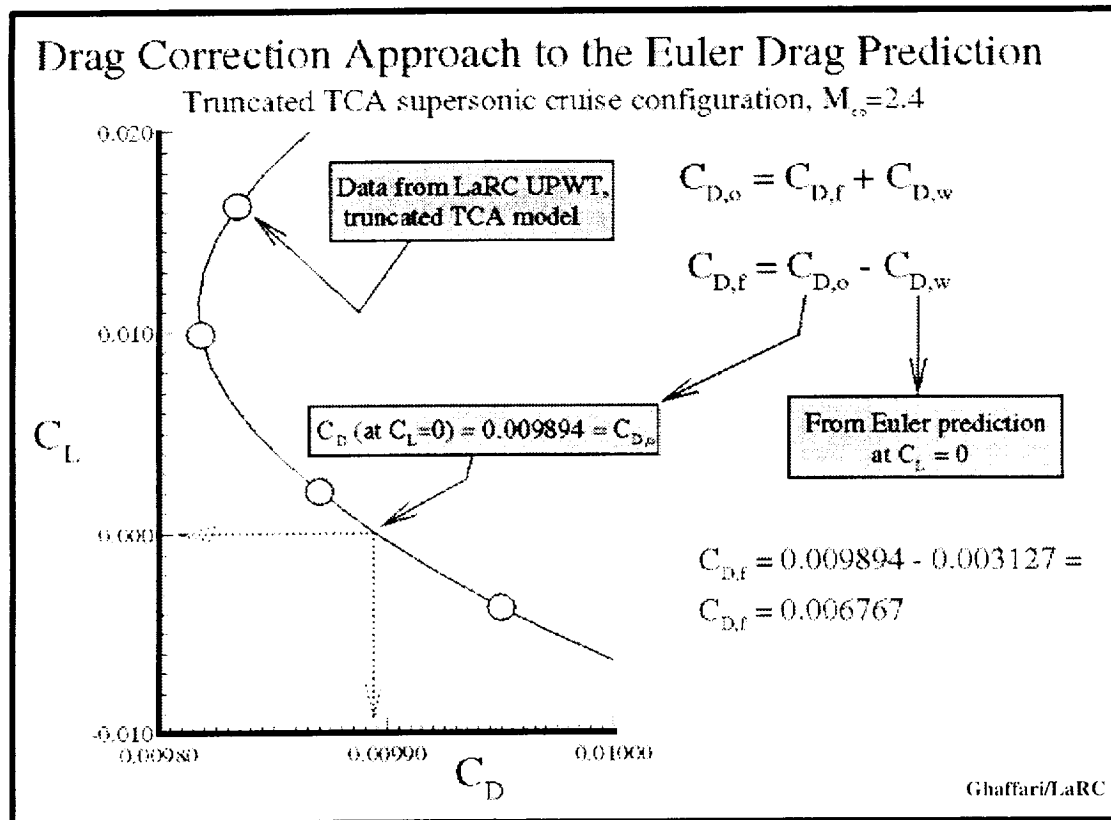
298

Surface Cp & Off–Surface Mach Predictions for the TCA
Flow through propulsion cruise geometry, Alpha=3.5°, Mach=2.4
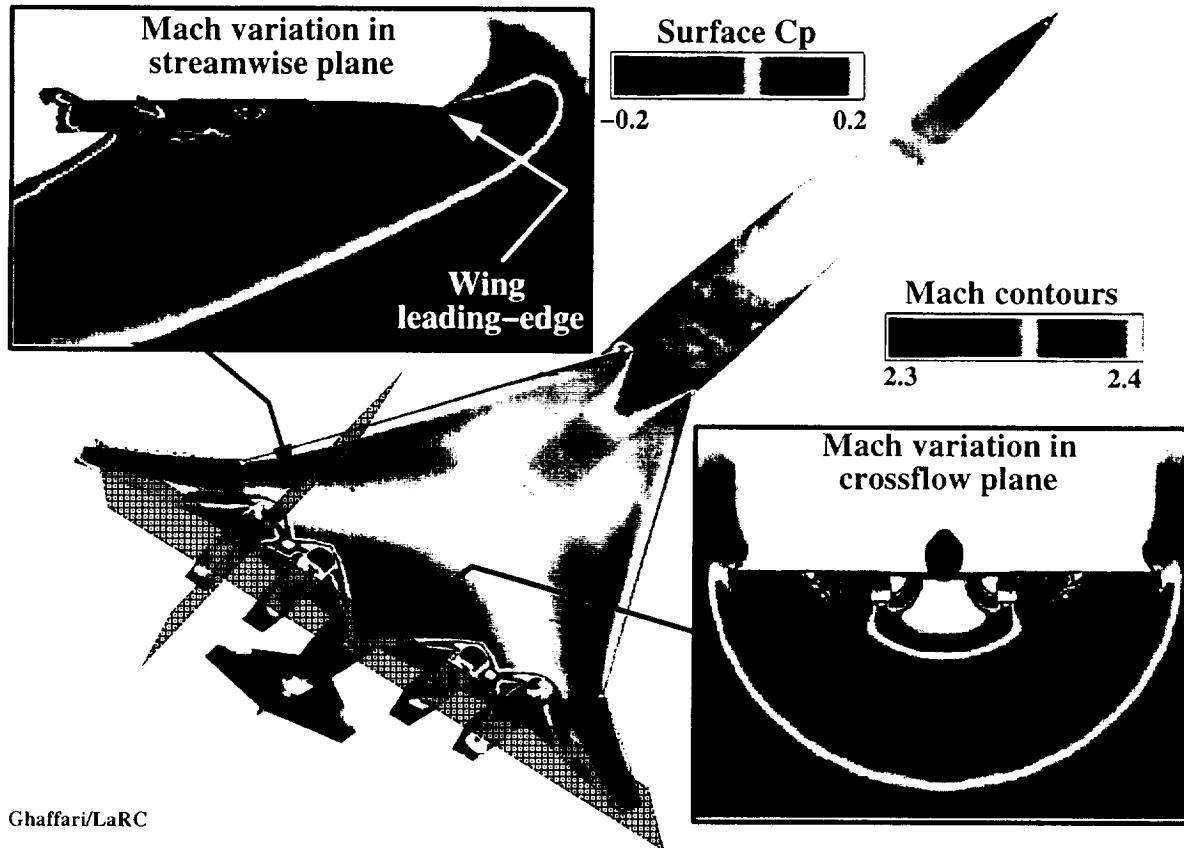
Typical off–surface flow features, highlighted by Mach number variation in a cross–flow & streamwise planes, in conjunction with the surface Cp distribution are shown in this chart for the complete TCA configuration. To accentuate the flow features in & around the nacelles, the Mach number variation in both the cross–flow & streamwise planes are contoured over a compressed range of 2.3 to 2.4. Over this contour range, the Mach numbers exceeding 2.4 (i.e., free–stream cruise Mach) are shown in white, while, Mach numbers below 2.3 are shown in black color indicating a slower moving flow relative to the free–stream.

The Mach variation in the cross–flow plane, longitudinally located slightly aft of the engine inlets, indicates a speed range in excess of the free–stream cruise Mach for essentially the entire upper surface and a region between the two inboard nacelles. The Mach variation in the cross–flow plane also indicates a compression region wrapped around the outboard nacelles and an extension toward the outboard wing leading–edges. Furthermore, the off–surface extension of the shock waves emanated from the inboard nacelle diverter (i.e., inboard legs close to the configuration plane–of–symmetry) is also shown to bend outboard and impinge on the exterior side of the inboard nacelles.
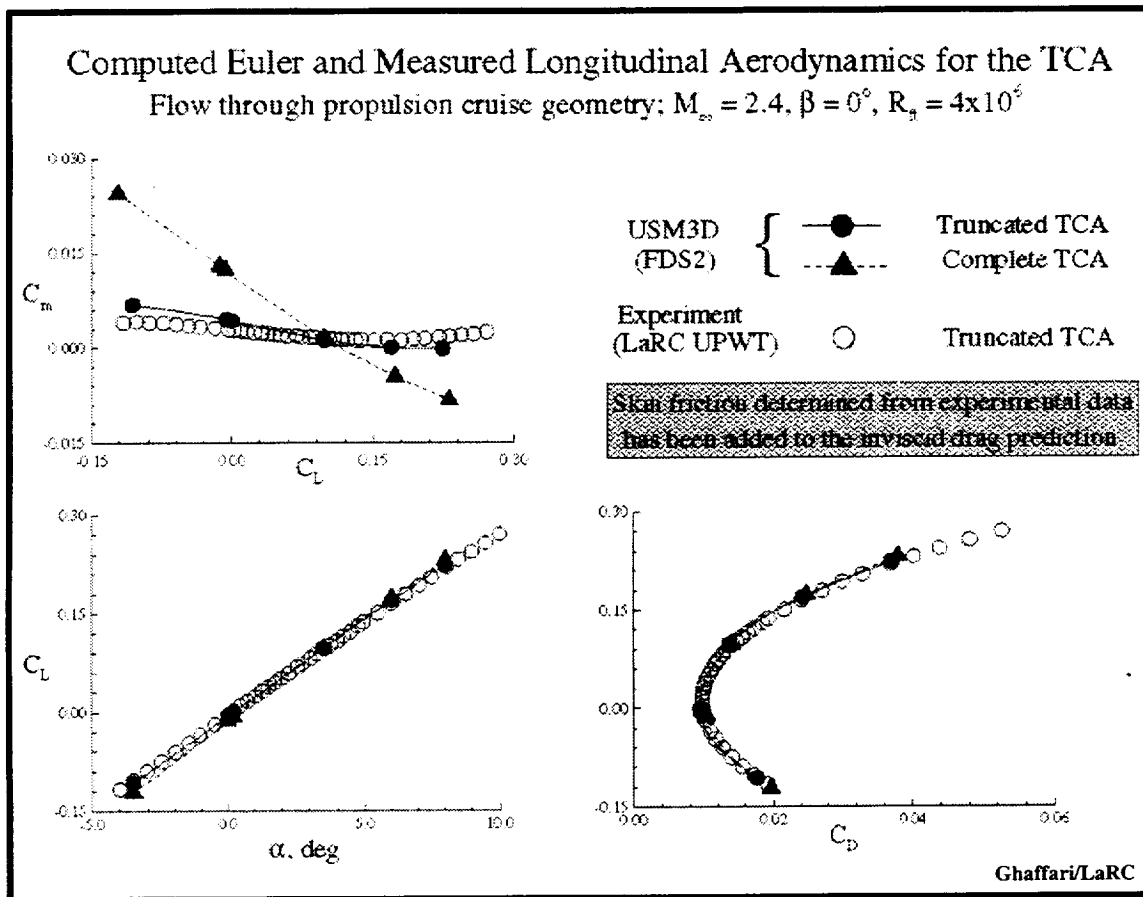
The Mach variation in the streamwise plane (parallel to the configuration plane–of–symmetry), located at a station that roughly cuts through the starboard mid–outboard nacelle is presented in the upper left of the figure. The Mach variation clearly shows a region of flow compression around the wing leading–edge followed by another one just ahead of the nacelle inlet. The outboard nacelle interior flow structure reveals a series of shock waves that bounce back and forth, creating regions of flow expansion and compression on the interior surfaces of the nacelle.

299

Drag Correction Approach to the Euler Drag Prediction

Truncated TCA supersonic cruise configuration, $M_{cr}=2.4$

Data from LaRC UPWT, truncated TCA model

$$C_{D,o} = C_{D,f} + C_{D,w}$$

$$C_{D,f} = C_{D,o} - C_{D,w}$$

C_D (at $C_L=0$) = 0.009894 = $C_{D,o}$

From Euler prediction at $C_L = 0$

$$C_{D,f} = 0.009894 - 0.003127 =$$

$$C_{D,f} = 0.006767$$

Ghaffari/LaRC

In general, there are two aerodynamic phenomena contributing to the total drag (C_D) force exerted on an airborne vehicle, the viscous (or the skin friction) component ($C_{D,f}$) and the pressure drag (or the drag–due–to–lift or vortex drag) component ($C_{D,p}$). In supersonic flow, the pressure drag consists of both the drag–due–to–lift ($C_{D,l}$) and the wave drag ($C_{D,w}$) components. Hence,

$$C_D = C_{D,f} + C_{D,p} = C_{D,f} + C_{D,l} + C_{D,w}$$

Conventional approach is taken to correct the drag coefficients predicted by the present Euler analysis to account for the viscous component of the total drag coefficient. This correction is required primarily due to the inviscid nature of the present Euler analysis and the inherent limitation of the corresponding equations to only predict the pressure components of the total drag. This conventional approach is based on determining the total drag coefficient at zero lift (i.e., $C_{D,o}$) using the experimental drag polar curve. This approach is adopted and the $C_{D,o}$ determined, as shown in the above plot, to be 98.94 drag counts. However, the determined $C_{D,o}$ is not only the drag contribution due to viscosity but it also includes the wave drag component. In an effort to isolate the wave drag component from the determined $C_{D,o}$, an Euler solution was obtained at an angle–of–attack of 0.2^{o} which was found to correspond to the experimental zero–lift data. It is assumed that the pressure drag coefficient predicted by the Euler method is solely the wave drag component with no contribution from drag–due–to–lift. The resulting wave drag coefficient is computed to be 31.27 counts. As a result, the skin friction contribution to the total drag can now be determined by subtracting the computed wave drag at zero lift from the determined $C_{D,o}$ as shown in the above figure. The skin friction coefficient, found to be 67.67 counts (assumed to remain constant with both the angle–of–attack and sideslip angle) is used to correct all the drag coefficient predictions in the present Euler analysis.

300

Computed Euler and Measured Longitudinal Aerodynamics for the TCA

Flow through propulsion cruise geometry; $M_\infty = 2.4$, $\beta = 0°$, $R_n = 4 \times 10^6$

The computed longitudinal aerodynamic characteristics are presented here for both the complete and the truncated TCA configuration, along with the measured experimental data for the truncated TCA model at supersonic cruise Mach number of 2.4. The results for the computed lift coefficients clearly indicate minimal effects due to the additional empennage loads at 3.5° alpha (i.e., close to the configuration design cruise angle–of–attack). However, as expected for off–design angles–of–attack, the additional load from the presence of the empennage on lift becomes more pronounced, i.e., increase in C_L for alpha > 3.5° and decrease in C_L for alpha < 3.5°. Although the latter effects on C_L are relatively small, the corresponding impact on the pitching moment is considerable due to the long moment arm. The results indicate that the additional load from the empennage presence to be minimal at the design cruise angle–of–attack of 3.5°, cause a pitch down for alpha > 3.5°, and cause a pitch up for alpha < 3.5°. Furthermore, the empennage load increments on the computed drag coefficients appear to be small over the examined range of flow conditions.

The correlation between the predictions and the experimental data for the truncated TCA configuration indicate good agreement for the pitching moment, lift and drag coefficients across the examined angle–of–attack range.

301

— Results & Discussion —

Longitudinal analysis

- **Typical flow features**
    - Surface pressure contours
    - Correlation with PSP data
    - Off–surface flow structures
- **Force & moment analysis**
    - Drag correction to Euler predictions
   - Correlation with data

Lateral/directional analysis

- **Typical surface pressure contours**
- **Forces & moments predictions – correlation with data**

Lateral/directional aerodynamic analysis is presented next which includes results for typical surface pressure contours followed by integrated forces/moments and correlations with experimental data.

Surface Cp Prediction for the Complete TCA Model
Flow through propulsion cruise geometry, Alpha =0°, Beta=3°, M=2.4

Surface Cp

−0.2   0.2
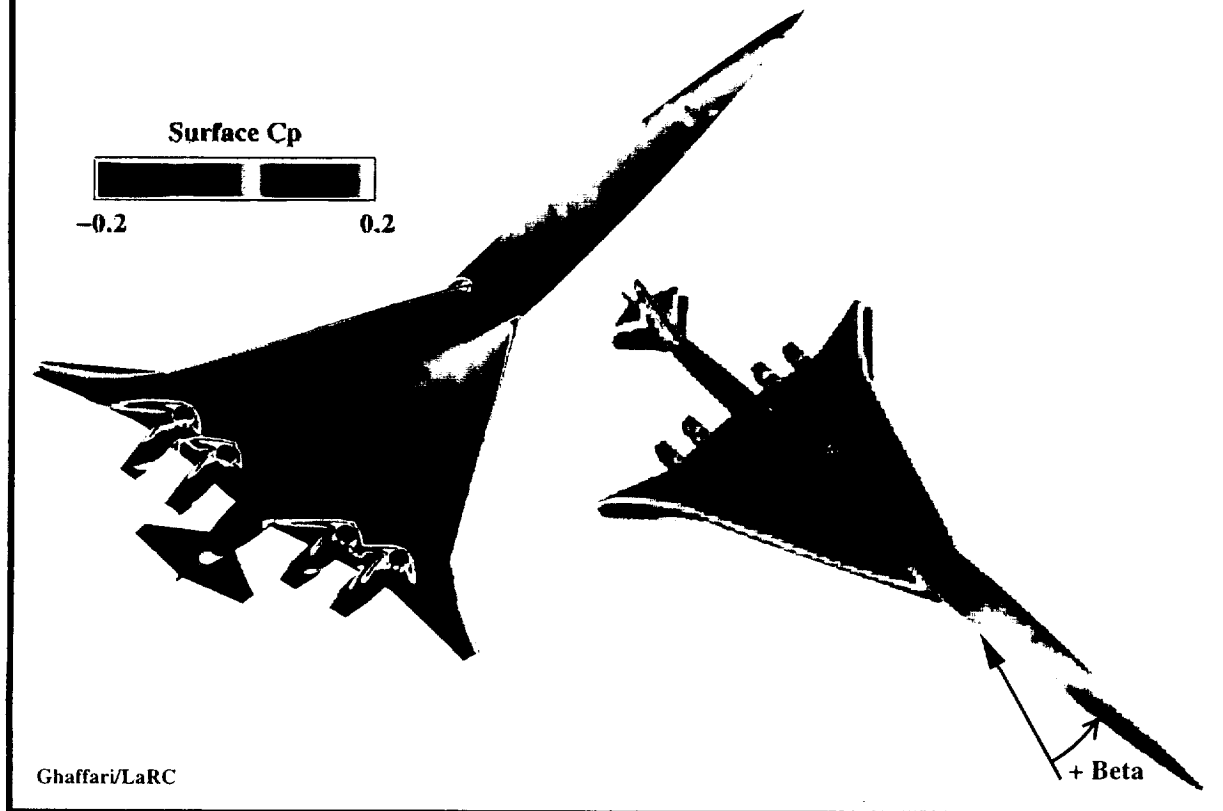
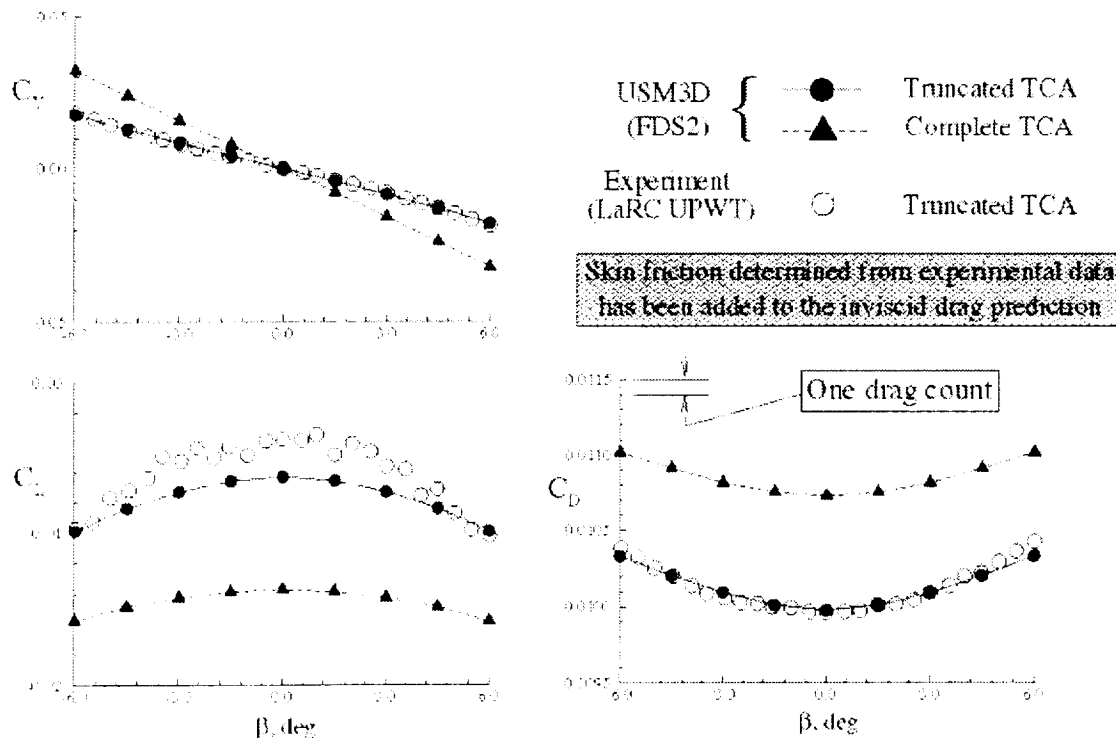Ghaffari/LaRC   + Beta

Typical upper & lower surface Cp contours computed at a finite sideslip angle are shown in this figure from similar vantage points and contour range consistent with the earlier results presented for the longitudinal analysis. The results clearly show the expected asymmetrical load distribution on both the upper and lower surface. The lower surface pressure contours indicate a region of expansion (Cp ~ −0.2) that runs roughly parallel to the starboard leading–edge of the inboard wing, whereas, the pressure contours around the port–side leading–edge of the inboard wing show a fairly benign attached flow condition. The upper surface Cp contours indicate a uniform distribution over the majority of the wing with a narrow band of compression along the starboard leading–edge of the inboard wing which expands over onto the outer wing panel. In addition, the computed upper surface pressure contours over the horizontal tails also show a large region of compression just aft of the leading edges, particularly on the starboard side.

303

Computed Euler and Measured Aerodynamic Forces at Sideslip for the TCA

Flow through propulsion for cruise geometry: $\alpha = 0°$, $M_\infty = 2.4$, $R_n = 4 \times 10^6$

The overall aerodynamic force characteristics computed for the complete TCA configuration across the examined range of sideslip angles at zero–degree angle–of–attack and supersonic cruise Mach number of 2.4 are shown in this figure. The experimental data for the truncated TCA model along with complementary results extracted from the full TCA numerical simulation (i.e., with appropriate component integration to only account for the truncated TCA geometry) are also included in the figure. Note the small scales in these plots, particularly in the measured lift coefficients which clearly illustrate the scattering of the data, as a function of sideslip angle, contributing to the overall asymmetrical lift distribution about the zero–degree sideslip angle (i.e., positive and negative sides).

The predicted side–force coefficients for the truncated TCA configuration are in excellent agreement with the experimental data, both in terms of magnitude and trends, across the examined range of sideslip angles. In general, the sideforce coefficients vary in a fairly linear fashion with sideslip angle and the corresponding change in the slope for the complete TCA configuration can mainly be attributed to the asymmetrical load distribution on the vertical–tail.

The computed lift coefficients for the truncated TCA configuration correlate very well with the measured data across the examined sideslip range. The presence of the empennage also appears to cause a nearly constant decrease to the overall lift coefficient for all the sideslip angles considered in the present study.

Similar to the lift coefficients, the computed drag coefficients for the truncated TCA configuration also correlate very well with the experimental data and that the empennage presence cause nearly a constant increase in the overall drag coefficients (~ 7 drag counts) across the examined sideslip angles.

304

Computed Euler and Measured Aerodynamic Moments at Sideslip for the TCA
Flow through propulsion cruise geometry; $\alpha = 0°$, $M_\infty = 2.4$, $R_{ft} = 4 \times 10^6$
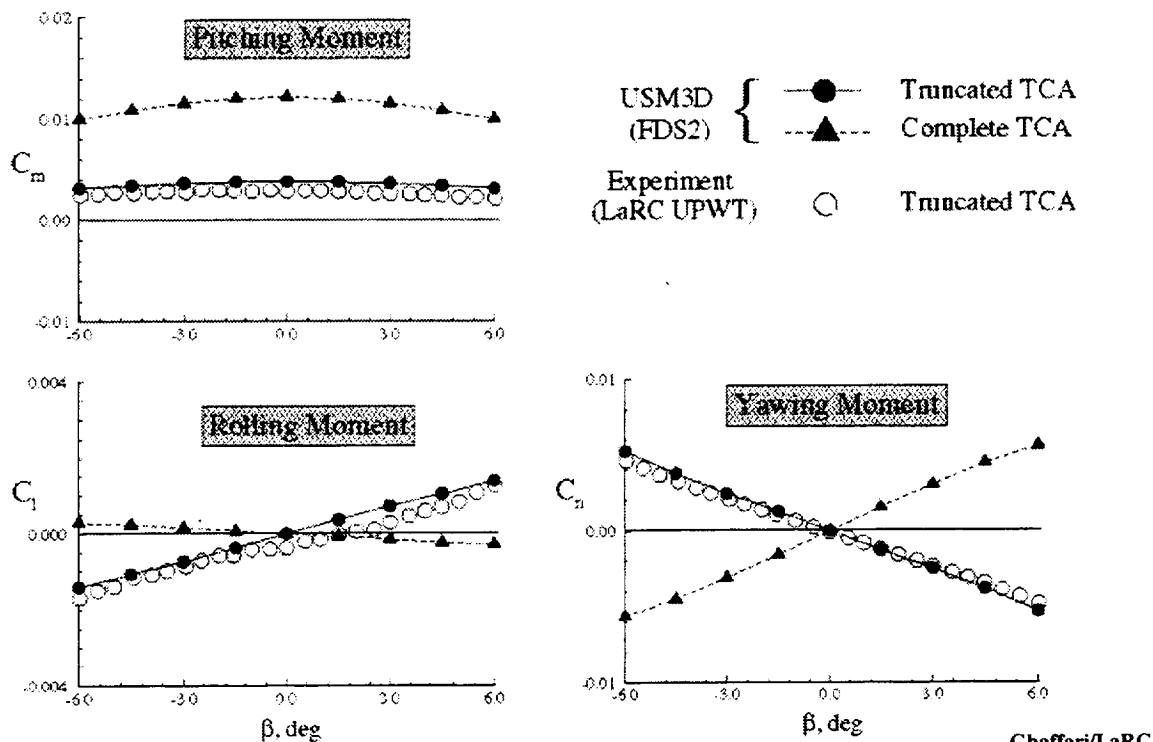
The computed and measured aerodynamic moment characteristics for the truncated TCA configuration across the examined range of sideslip angles are presented in this figure. Complementary numerical predictions for the complete TCA configuration are also included for comparison. In general, there is an excellent correlation between the numerical predictions and the measured data for the aerodynamic moment characteristics of the truncated TCA configuration across the examined range of sideslip angles. As expected, the aerodynamic moments predicted for the complete TCA configuration clearly indicate a dramatically different characteristics than those of the truncated TCA model. These differences in the moment characteristics are primarily due to the presence of the empennage components. For example, the results indicate a sign reversal in the yawing and rolling moments which can primarily be attributed to the presence of the vertical and horizontal tails. Furthermore, the pitch–up moment characteristics for the complete TCA configuration can be mainly be attributed to the negative load contributions due to the empennage presence. It should also be noted that the asymmetrical lift distribution in the measured data, for positive and negative sideslip angles discussed in the previous chart, is the primary cause of the nonlinearities in the rolling moment distribution. Such nonlinearities in the measured rolling moment distribution are evident as they deviate from a fairly linear character of the computed results, in particular, around zero and the positive sideslip range.

305

— Concluding Remarks —

● **TCA longitudinal aerodynamic characteristics for supersonic cruise are accurately predicted by the present unstructured grid Euler method**

● **TCA lateral/directional aerodynamic predictions agree very well with experimental data**

● **Predicted nacelles shock–wave structures correlate reasonably well with Pressure Sensitive Paint data**

● **Computational method produced consistent results across the examined range of conditions without any convergence difficulties**

● **Completed the documentation – Presently being reviewed**

What's next?

The numerical results clearly demonstrate that the present unstructured grid Euler method is a viable tool that can be used, with confidence, for the aerodynamic analysis of the high–speed–civil–transport class of vehicle in the early configuration design cycle. The present analysis also indicates that the method is robust and produces consistent solutions across the examined range of flow conditions without any convergence difficulties. Where would we like to go next from the present Euler analysis?

Well, to Navier–Stokes flow simulation.

306

Surface Cp Prediction for the Complete TCA and Correlation with PSP
Unstructured Grid Method (TetrUSS); M = 2.4, Alpha = 3.5°, $R_{ft} = 4 \times 10^6$
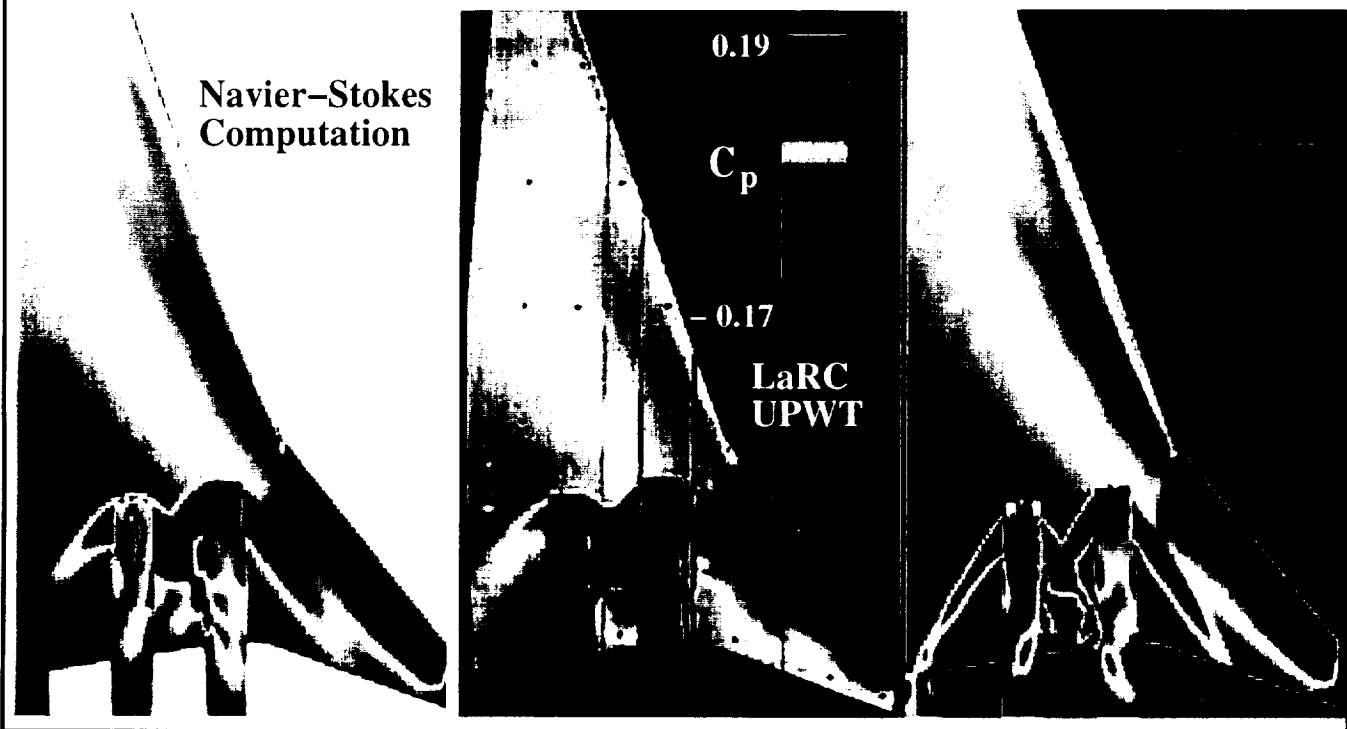
The lessons learned from the present Euler analyses were used to extend the computations to simulate the viscous flow over the same configuration for cruise conditions. Advancing–layers method was used to add grids in the viscous region to resolve the boundary–layer flows. This effort has already been initiated and preliminary results indicate good correlations with experimental data. A representative result for the computed wing lower–surface pressure distribution is shown here to complement the present Euler analysis. The Navier–Stokes result clearly show an improvement over the Euler flow predictions for simulating the shock waves around the nacelles. Also note that the viscous effects appear to have minimal impact on other regions of the wing lower–surface pressure distribution.

307

This page is intentionally left blank.